https://ntrs.nasa.gov/search.jsp?R=19840003616 2020-03-21T01:44:30+00:00Z

View metadata, citation and similar papers at core.ac.uk

brought to you by CORE

provided by NASA Technical Reports Server

General Disclaimer

One or more of the Following Statements may affect this Document

- This document has been reproduced from the best copy furnished by the organizational source. It is being released in the interest of making available as much information as possible.

- This document may contain data, which exceeds the sheet parameters. It was furnished in this condition by the organizational source and is the best copy available.

- This document may contain tone-on-tone or color graphs, charts and/or pictures, which have been reproduced in black and white.

- This document is paginated as submitted by the original source.

- Portions of this document are not fully legible due to the historical nature of some of the material. However, it is the best reproduction available from the original submission.

Produced by the NASA Center for Aerospace Information (CASI)

(NASA-TM-85093) REPORT OF THE FIRST NIMBUS-7 SMMR EXPERIMENT TEAM WORKSHOP (NASA) 25 p HC A02/MF A01 CSCL 08L

N84-11684

Unclas
G3/48 42433

NASA

Technical Memorandum 85093

Report of the First Nimbus-7 SMMR Experiment Team Workshop Held at Goddard Space Flight Center on October 28-30, 1982

W. J. Campbell and P. Gloersen

NOV 1983
RECEIVED
NASA STI FACILITY
ACCESS DEPT.

August 1983

National Aeronautics and
Space Administration

Goddard Space Flight Center
Greenbelt, Maryland 20771

CONTENTS

1. Introduction

2. Algorithm Comparison

2.1 SMMR Team Algorithm

2.1.1. Description

2.1.2. Results

2.1.3. Limitations

2.1.4. Immediate adjustments

2.2 AES Algorithm

2.3. NORSEX Algorithm

3. Emissivity

4. SMMR and Arctic Ocean Buoy Program

5. Conclusions and Recommendation

6. References

7. List of Figures

8. Appendix A -- List of Participants

1. INTRODUCTION

For the past several years, members of the Nimbus-7 Scanning Multichannel Microwave Radiometer Experiment Team (SMMR/NET) have discussed the need to compare SMMR sea ice results with various in-situ and aircraft observations carried out independently by other scientists. During the last few years, some important data sets of this nature have been acquired in the Greenland, the Beaufort, and the Bering Seas. Thus. it was decided to hold a SMMR sea ice workshop at NASA Goddard Space Flight Center on 28-30 October, 1982 following a regular SMMR/NET meeting. The list of participants who attended this meeting are given in Appendix A.

The objectives of this workshop were as follows: (1) to evaluate and compare the sea ice parameter retrieval algorithms developed by the SMMR/NET, the Norwegian Sea Remote Sensing Experiment (NORSEX) group, and the Canadian Atmospheric Environment Service (AES); (2) to recommend possible improvements to the SMMR/NET sea ice algorithm for processing SMMR data acquired for the subsequent archival year; and (3) to define SMMR-related analyses to be performed during the coming year to aid in the determination of possible refinements in that algorithm for subsequent archival years.

The comparisons of sea ice concentrations and multiyear fractions derived from SMMR radiances with independent data sets, such as the AES Ice Reconnaisance sea ice maps of the Beaufort Sea, clearly showed that the SMMR makes accurate global measurements of these parameters. The multispectral capability of SMMR has led to significant improvement in the mapping of sea ice concentration, e.g. over Nimbus-5 ESMR and other sensors. The first routine global mapping of multiyear ice fraction (the amount of ice present that is multiyear) has been demonstrated. Considerable enthusiasm was expressed for the value of SMMR sea ice observations for scientific studies and operational ice mapping. Nevertheless, in certain cases, substantial seasonal and regional differences were noted between the SMMR/NET algorithm, which was developed for operational use on a global basis, and the other regional algorithms. Comparisons of certain in-situ and aircraft data sets have verified the anticipated limitations of the SMMR/NET production algorithm during sea ice melt periods. Much of the workshop was devoted to outlining the steps for further evaluation of each of the algorithms.

The participants decided to meet annually in the fall or winter to review work accomplished in the preceding year and to determine if further refinements are necessary to the SMMR/NET sea ice algorithm. They also decided to call themselves The SMMR Sea Ice Working Group.

2. ALGORITHM COMPARISONS

2.1. SMMR Team Algorithm

2.1.1. Description

The physical basis of the SMMR sea ice algorithm derives from both

the polarization and spectral characteristics of sea water and various ice types within the field-of-view of the instrument. At present the algorithm determines ice concentration, multiyear ice fraction and sea ice temperature.

The effective emissivities which are implicit in the SMMR Team algorithm are presented in Table 1. Calm sea water at a temperature of 271K, first-year, and multiyear ice at each of the five SMMR channels are compared with the corresponding emissivities determined from the other groups. Important features to note include: water emissivitites are consistently lower than those of either of the two ice types; ice emissivities generally either remain constant or increase with wavelength while water values decrease; ice exhibits a smaller degree of polarization than does water at all wavelengths; largest contrast between water and ice occurs at the longest wavelenghts while the greatest contrast between ice types occurs at the shortest wavelengths.

The SMMR Team algorithm utilizes various radiance ratios to obtain the ice parameters. Through the use of these ratios, the effect of changes in sea ice temperature is greatly reduced. This is expected to improve the accuracy of the retrievals without the need either to continously monitor surface radiating temperatures which depends on the availability of surface data, as, for example, provided by the Arctic Ocean Buoys, or to use climatological surface temperature values as was done with the ESMR-5 sea ice algorithm (Zwally et al.,1982). The ice concentration depends primarily on the observed polarization of the surface, which is defined by:

$$PR = (TB(V)-TB(H))/(TB(V)+TB(H))$$

for the 0.81 and 1.7 cm SMMR wavelengths used to obtain ice concentration estimates at the 30 and 60 KM SMMR cell resolution. The form of the equation relating concentration to polarization is:

$$C = (a1+a2*PR)/(a3+a4*PR)$$

where the a's depend on the radiances of the tie-points chosen for the various surface components within the FOV and also partly on the multiyear fraction F. It should be emphasized that actual emissivities were used in the algorithm for processing only the first-year data set; in subsequent years, the algorithm was "tuned" by selection of appropriate tie-points for FY, MY, and open water (Cavalieri et al., 1984).

The determination of the multiyear fraction makes use of the spectral difference between the first-year and multiyear ice components as defined by the 0.81 and 1.7 cm vertical gradient ratio. This ratio is:

$$GR = (TB(.81V)-TB(1.7V))/(TB(.81V)+TB(1.7V))$$

The expression relating the multiyear fraction to the gradient ratio is:

$$F=(b1+b2*GR)/(b3+b4*GR)$$

where the b's depend on the tie-point radiances and partly on the total ice concentration C.

Table 1.

SMMR Channel		Source*	Emissivities		
			Open Water	FY Ice	MY Ice
6.6	H	J		.87 ± .02	.82 ± .03
	V	SMMR	.53	.99	.96
	V	J		.93 ± .02	.88 ± .03
10.7	H	N	.281 ± .010	.880 ± .046	.112 ± .058
		J		.88	.80
	V	N	.545 ± .010	.939 ± .014	.886 ± .058
		J		.93 ± .02	.86 ± .03
18.0	H	AES	.42	.89	.80
		J		.88	.75
		SMMR	.38	.94	.80
	V	AES	.61	.93	.86
		J		.92 ± .03	.80 ± .03
		SMMR	.62	.98	.86
21.0	H	N	.354 ± .010	.906 ± .025	.635 ± .125
		J		.89 ± .04	.74 ± .05
	V	N	.633 ± .015	.953 ± .003	.787 ± .080
		J		.92 ± .04	.77 ± .05
37.0	H	N	.387 ± .012	.904 ± .021	.582 ± .068
		AES	.52	.88	.69
		J		.88 ± .03	.66 ± .03
		SMMR	.49	.92	.68
	V	N	.685 ± .94	.945 ± .001	.675 ± .075
		AES	.72	.92	.72
		J		.92 ± .03	.71 ± .03
		SMMR	.73	.96	.71

*J - Values obtained from analysis of SMMR/TH IR data.

SMMR - Values corresponding to the tie-point radiances currently used in the SMMR NET operational algorithm obtained by dividing these radiances by the corresponding SMMR and Arctic Ocean Buoy temperature data. (The ocean tiepoint results from a model calculation.)

N - Values obtained from NORSEX field measurements.

AES - Values obtained from SMMR and weather station temperature data.

Finally, the ice temperature is computed at the 150 KM SMMR resolution from the following expression:

$$Tice=((4.6V)-271*(1-C)*EOV(4.6))/EFV(4.6)*C$$

where 4.6V is the 4.6 cm vertical brightness temperature, EFV(4.6) the first-year ice vertical emissivity at 4.6 cm, and C the total ice concentration at 60 KM averaged over a 4.6 cm footprint.

The algorithm is diagrammed in Figure 1. The 4.6(V), 1.7(H&V), and 0.81(H&V) cm brightness temperatures are input into the algorithm. Following computation of the polarization and gradient ratio, an iterative technique is used to obtain estimates of ice concentration and multiyear ice fraction. The ice concentration is then used to infer the physical ice temperature from the 4.6 cm vertical brightness temperature.

A comparison of the values obtained using this algorithm and Nimbus-7 SMMR data acquired during the NASA CV-990 underflights with similar information derived from the airborne multispectral radiometer data is shown in Figure 2. In that figure, the ice parameters, total concentration and multiyear ice concentration, are calculated from airborne radiometric data consisting of horizontal and vertical polarizations at wavelengths of 0.8 and 2.8 cm, using the same algorithm as for the spacecraft data but different tie-points to accommodate the different wavelengths, view angles, and radiometer calibrations of the airborne sensors. (2.8 cm data were used since the 1.7 cm radiometer was not operational during these flights.) The data were acquired east of Greenland near local noon (GMT is shown) on 6 November 1978, corresponding closely to the Nimbus-7 overpass. The corresponding data from the Nimbus-7 SMMR are shown as dashed lines. There is a convincing similarity between the two retrievals (taking into account the "washing out" of features in the larger-footprint data from the Nimbus-7 SMMR). Particularly striking is the comparison of the two data sets on the southbound leg (after "1" on the figure) where the total ice concentration remains at about 75% along that leg whereas the multiyear sea ice concentration is reduced by about a factor two.

Figure 3. shows an example of a histogram made from a north polar stereographic projection (50 degrees N to the pole) of the total ice concentration retrieval at the 60 KM resolution. The polar image (not shown) represents an average ice concentration over a five-day period beginning February 3, 1979. The histogram indicates two peaks. The ice peak is centered on 102% and the ocean peak on 6%. The width of the ice peak at half maximum is 9% or approximately +/- 5% about the maximum. This is a measure of the relative uncertainty in the concentration determination. It includes, of course, the real variability of ice concentration but it also places an upper limit on the precision of the retrievals. The ocean peak at 6% illustrates the effect of both the wind-roughened surface and the atmospheric burden on the concentration retrievals. If desired, the ocean peak may be adjusted to 0% either by adjusting the zero-point ocean radiances or by simply making a scale adjustment.

The histogram shows that the concentration retrievals are quite reasonable for the entire north polar region. Individual case studies

comparing the SMMR retrievals with independent measurements are needed to provide a determination of the accuracy of the retrievals for various seasons and regions.

Table 2. summarizes the histogram analysis statistics for the first 11 months of SMMR data. Each histogram is based on a five-day average for each month from November 1978 through September 1979. Listed in the Table are the ocean peak, ice peak, ocean minimum and ice maximum concentrations. The ocean peak varies between 2 to 8% with an 11-month average close to 6%. During the winter months the ice peak is typically 98% to 102% with lower values during the summer months. These lower values are for the most part a result of the different ice surface characteristics due to surface melting including the effects of wet snow cover and the presence of melt ponds. Ocean minimum concentration is essentially 0% and the ice maximum generally averages about 110%. Concentration values above 100% and some fraction below 100% represent variations due to the differences between the actual brightness temperature within the field of view of the instrument and that assumed for a given ice type. This includes implicitly ice types present but neglected in the algorithm such as new, young, and second-year ice types.

Table 2.1 Summary Statistics of Histograms Analysis

Date	Total Ice Concentration (60 km)			
	Ocean Peak	Ice Peak	Ocean Min.	Ice Max.
308-310 1978	8%	100%	0%	110%
339-343	8%	98-102%	0%	110%
4-8 1979	6%	102%	0%	110%
34-38	6%	102%	0%	112%
64-68	6%	102-104%	0%	114%
94-98	4%	102%	0%	114%
130-134	2-4%	102%	0%	114%
184-188	8%	88-96%	0%	116%
208-212	6%	84-86%	2%	106%
232-236	8%	90-92%	0%	108%
256-260	8%	92-98%	0%	104%

2.2. Cal Swift/AES Algorithm

Comparisons were made between the results of the Team algorithm (Parm tapes) and the Atmospheric Environment Service (AES) ice charts for the Southern Beaufort Sea and the Gulf of St. Lawrence. For the Beaufort Sea in areas of 100% first-year ice, the Team algorithm gave good results with concentrations of 90-99%. For multiyear ice areas further north the Team multiyear fractions were of the order of 80%. Since insufficient observations are available it is difficult to provide a comparison with ice charts originating from the various ice centres (e.g. AES, Joint Ice Centre (Navy/NOAA)). These ice centres call any concentration of pack ice containing multiyear ice concentrations greater than 35% as 90 plus % MY concentration. In comparing the results with the Cal Swift/AES algorithm these regions gave 99% MY ice fractions as expected from past historical records.

For the Gulf of St. Lawrence and Labrador Sea area, the archival sea ice parameter data tapes do not provide any ice information below 50 degrees North. In areas of open water, as seen on the AES ice charts, the Team algorithm gave ice concentrations between 10 and 25% and in fact gave no indication of any ice edge being present. This was observed for both clear and cloudy days. Concentrations within the ice pack itself ranged from 60-99%, whereas the AES ice chart showed this region to be 90+% covered by first-year ice. The archival tape data also showed multiyear ice concentrations of the order of 25% in the Labrador Sea. AES ice charts show no presence of multiyear ice in this area.

The development of this algorithm was motivated by a desire to retrieve ice/water fractions from SMMR data with minimal computational requirements. To this end, all terms in the radiative transfer equation were linearized to include only a nominal polar water vapor correction. Attenuation and emission from the clouds were ignored under the assumption that clouds in the high Arctic consist of low attenuating ice crystals. Under these assumptions, the resulting unknowns are emissivity and physical temperatures. This algorithm requires physical temperature as a priori known (or guessed) parameter. Retrieved surface temperature was not used because it was believed that such an algorithm would utilize the 6.6 GHz channel, whose footprint is too large to provide satisfactory results on a finer spatial scale. The emissivity at each frequency and polarization is also required and is linearly retrieved from the respective brightness temperature measurement. Under the constraint that the sum of all the fractions add to unity, fraction multiyear ice, fraction first-year ice and fraction water are retrieved from a minimum of two channels. Combinations of 18 GHz and 37 GHz channels are utilized to give the best possible spatial resolution. The 21 GHz channel was not selected because of potential errors introduced by water vapor; however, it will be woven into the algorithm at some future date for purposes of atmospheric correction or to flag data contaminated by the atmosphere.

The equations that are used for retrievals of the three fractions are explicitly given in Figure 4. In these equations, T_B^{18} and T_B^{37} are input values of the brightness temperatures (either polarization) and the "E" is the emissivity of the various wavelengths, polarizations, and ice types of interest.

2.3. NORSEX Algorithm

The NORSEX algorithm has been developed for estimating total and multiyear ice concentration from SMMR data with input of surface air temperature measurements. The radiation model is composed of two main parts, a model of the surface and a model of the atmosphere above. Also, radiation from free space gives a minor contribution (Svendsen et al., 1983, in press).

In the retrievals, surface-measured emissivity spectra of multiyear ice, first-year ice and calm cold sea water (NORSEX Group, 1982) is used (Figure 5.). From these spectra it is seen that due to the large difference between mulityear ice and first-year ice at 37 GHz, this choice of frequency to separate the two ice types provides the greatest sensitivity. Furthermore, the spectra indicate that to separate ice from water, in addition one of the lower frequencies must be used, giving the best accuracy but unfortunately the worst spatial resolution for the lowest frequency. Studies of horizontally polarized SMMR data (TCT data) from far into the ice pack showed unexplained variations and offsets and therefore we exclude all horizontal channels when computing ice concentrations.

Based on this information, the combination of 10V/37V is chosen for estimates of total and multiyear ice concentration, but comparable estimates from the combination 18V/37V are also made to give better spatial resolution. The algorithm is dependent on well-calibrated values for brightness temperatures. Therefore, in orbit calibration of SMMR data over calm open water (cold calibration point) is performed and we assume the prelaunch black-body calibration is good.

The algorithm consists of the following computational steps:

1) The available SMMR data are adjusted to give "calibrated" brightness temperatures at satellite height T_M.

2) An initial correction to T_M for atmospheric effects is performed using an atmospheric model using surface air temperatures measured from Arctic Ocean Buoys.

3) Initial concentrations are computed.

4) A refined atmosphere is found by using initial total ice concentrations to interpolate between an atmosphere corresponding to the marginal ice zone and atmosphere corresponding to the deep pack ice (Reeves, 1925).

5) Using the refined atmosphere, final values for the concentration are computed.

Figure 6. shows maps of retrieved total and multiyear ice on October 11, 1979 north of Svalbard. On the maps are shown the best estimate of the position of the ice edge (accuracy +/- 10 km NORSEX Group 1982), taken from the maximum of the 37 H channel which coincides very well with the 45% total ice concentration isoline (not shown in the figures). Also the

well-known low concentration area near Greenland is seen (Koch, 1945). On the figures are shown the flight paths from the C-130 the day before, doing multichannel microwave measurements. On this day, the air temperature was approximately -9°C from these measurements. Concentrations are computed and compared with the NORSEX algorithms and the Team algorithm used on the SMMR data along the same lines (Figures 7 and 8). The accuracy of the aircraft measurement (compared with aerial photos) are estimated to be + 3% for total ice and + 10% for multiyear ice. On average the NORSEX algorithm gives SMMR concentration estimates within these uncertainties, while the Team algorithm gives total ice estimates 10-20% lower. The Team algorithm does however, as pointed out earlier, give self-consistent results in the central Arctic, and is in agreement with airborne observations in that region.

More aircraft measurements are needed to check the validity of the estimates at different times of the year and in different regions.

3. Emissivity

Table 1. compares the emissivities derived by three different methods. While the SMMR Team Algorithm does not use emissivities explicitely, the emissivities corresponding to the radiative tie-points were obtained by dividing those radiances by the Arctic Ocean Buoy Temperature data, which provides an interpolated temperature field using also the weather station data. The buoy temperature is an integrated ice, snow, and air temperature as well as the effects of long and short radiative fluxes and cooling by the wind. (Thorndyke and Colony, 1980). The buoy temperature is reported to have been within a few degrees of the ambient air temperature (Martin and Clark, 1978). The radiances were obtained from the NIMBUS 7 Cell tapes. Both are averaged over an area of approximately 600 km by 600 km and over an average of 3 data days. This was done for MY ice using a region northwest of Greenland and for FY ice in a region over Baffin Bay. The open water emissivities were modeled values based on surface and atmospheric conditions. The atmospheric condition assumed zero cloud liquid water, 0.5 cm of atmospheric water vapor and a 7 m/s near surface wind.

The AES group used the interpolated temperature field based on the weather station data. The station data was then taken to model an ice-snow interface temperature (Ref. by Ramseier). The TB's were obtained from the NIMBUS-7 cell tapes. An emissivity was calculated by dividing the averaged cell tape temperature by the snow-ice interface temperature both averaged over an area of 400 by 400 km and over one data day. This was done for MY ice using a similar region as the team algorithm area. For the FY ice, the region included areas in Hudson Bay and the Gulf of St. Lawrence. The open water emissivities were obtained on a calm and clear day over the Scotian shelf.

Emissivities have also been determined, in a separate study (Comiso, 1983) using near simultaneous observations of the SMMR and the

Temperature Humidity Infrared Radiometer (THIR) sensors both on board the Nimbus 7 satellite. The snow/ice interface temperature is inferred using the THIR 11.5 micron-channel and a snow-ice interface model (Maykut and Untersteiner, 1971). This model is also compared and is in good agreement to a least squares fit to the Pond Inlet observations (Ramseier, private communications) as shown in Figure 9. Cluster analysis using a combination of different frequencies and polarization is used to isolate the ranges of values of the first-year and multiyear ice emissivities. Three large-scale areas are chosen (Chukchi Sea, Central Arctic, and Greenland Sea regions) during a winter day (February 25, 1979). The emissivities listed for first-year ice are near maximum values in the first-year ice clusters and are consistent with the AES values. For multiyear ice, the weighted average of the apparent multiyear ice clusters are chosen. However, there is large spatial variability in the observed multiyear ice values especially at 37 GHz. A cluster of emissivities with values between those of first-year ice and multiyear ice is prominent in the central Arctic. Some possible interpretations of these observations, which require further investigation, include the presence of second-year ice, first-year ice with thick snow cover, or mixtures of first-year and multiyear ice.

4. SMMR AND THE ARCTIC OCEAN BUOY PROGRAM

The Arctic Ocean Buoy Program provides important data for SMMR studies for testing and developing various sea ice and ocean algorithms and helping to insure the full utilization of the archived SMMR data set. The buoy program provides critical synoptic data on a continuous basis on surface air temperature, surface atmospheric pressure, and ice drift. This unique system has been in operation almost since the launch of SMMR on the Nimbus-7 satellite. The future funding for this system is in question, and there are strong arguments for continuing to operate this system during present and future multispectral microwave observations from space.

The buoy surface air temperature observations are used: (1) to test the distribution of radiating temperatures derived by some algorithms; (2) as required inputs to other sea ice algorithms; (3) and to improve our knowledge of microwave emissivities of sea ice. For example, the Nimbus-7 SMMR Experiment Team sea ice algorithm infers the radiating temperature of the ice, whereas the NORSEX algorithm requires the input of buoy temperature data for accurate retrievals. All existing algorithms have difficulty in distinguishing various ice types and concentrations when the ice nears its melting point due to nonlinear variation of the microwave emissivity of sea ice under those conditions. In fact, false retrievals for these parameters will occur under these conditions. Therefore, the buoy data are the only reliable means by which such conditions can be observed.

The Arctic Buoy Program provides the only accurate data on the distribution of atmospheric surface pressure over the Arctic Ocean. These data are now used to infer the fields of wind stress acting on the ice canopy, since the wind stress is the key driving force for the ice motion in the Arctic basin. The derived wind stress measurements are essential for ice dynamics model studies. These models, in turn, can

provide important information on the temporal and spatial variations of the ice concentration for comparison with ice concentrations derived from SMMR data. Coupled ice buoy drift and SMMR data may provide sigificantly improved estimates of new sea ice production, heat budget, and ice deformation.

5. Conclusion and Recommendations.

From the results presented here, it is evident that the various groups used different and independent approaches in deriving sea ice emisssivities and algorithms. In order to compare the different algorithms it is necessary to use a common set of emissivities. Therefore the SMMR Sea Ice WG has defined the following procedure to validate the SMMR Team algorithm.

a) To develop a common set of emisssivities the WG has defined the following regions for determining the beam-filling ice type and ocean emissivities;

MY - Ice region 79 to 84 deg North and 115 to 130 deg West for day 42(11 Feb 1979).

FY - Ice region 70 to 73 deg North and 165 to 175 deg West for day 338 (4 Dec 1979).

Ocean region 41 to 44 deg North and 50 to 60 deg West for day 64 (5 Mar 1979).

b) It was agreed to determine a radiative temperature by using the interpolated Arctic Buoy temperature data which includes the station data averaged over these regions and a snow-ice interface model (Ramseier). The brightness temperatures from the cell all tapes will be averaged over each of the corresponding areas and days. For computing the open ocean emissivities the surface temperature will be obtained from ship data.

c) The sea ice group of the SMMR NET Team has defined 2 months as a baseline data set for testing Team and alternate algorithms discussed above. March 1979 was picked as a typical midwinter month for which we have extensive surface and aircraft observations in the Beaufort and Bering Seas (SURSAT Proceedings, 1981; PMEL and UOW). October 1979 was chosen as representative of a transition month for which Arctic ocean buoy, Beaufort and NORSEX field observations are available.

d) Based on the results of the sea ice algorithm retrievals the SMMR NET Team will recommend appropriate sea ice algorithm modification to process the second year SMMR sea ice parameters.

6. REFERENCES

Cavalieri, D.J., Gloersen, P., and Campbell, W.J., Determination of Sea Ice Parameters with the Nimbus-7 SMMR, submitted to J. Geophys. Res., 1984

Comiso, J.C., Sea ice effective microwave emissivities from satellite passive microwave and infrared observations, J. Geophys. Res., 88, 7686-7704, 1983.

Gloersen, P. D. Cavalieri, A.T.C. Chang, T.T. Wilheit, W.J. Campbell, O.M. Johannessen, K.B..Katsaros, K.F. Kunzi, D.B. Ross, D. Staelin, E.P.L. Windsor, F.T. Barath, P. Gudmandsen, E. Langham, and R.O. Ramseier, A Summary of Results from the First Nimbus-7 SMMR Observations, submitted to J. Geophys. Res., 1984.

Maykut, G.A., and N. Untersteiner, Some Results from a Time-Dependent Thermodynamic Model of Sea Ice, J. Geophys. Rev. 76, 1550-1575, 1971.

Svendsen, E., Kloster, K., Farrelly, B., Johannessen, O. M., Johannessen, J. A., Campbell, W. J., Gloersen, P., Cavalieri, D., and Mätzler, C., Norwegian Remote Sensing Experiment: Evaluation of the Nimbus-7 Scanning Multichannel Microwave Radiometer for Sea Ice Research, J. Geophys. Res., vol. 88, 1983.

7. List of Figures

1. Diagram of SMMR/NET sea ice parameter retrieval algorithm for computing total ice concentration (C), fraction of ice that is multiyear (F), and radiating temperature of the ice.

2. Comparison of Nimbus-7 SMMR and airborne SMMR Simulator retrievals of total ice concentration (C), and multiyear ice concentration (C*F) in the marginal ice zone of the Greenland Sea along a CV-990 flight track during the SMMR Underflights Mission in November 1978.

3. Histogram of ice concentration retrieval values in the Arctic.

4. The Cal Swift/AES sea ice parameter retrieval algoithm.

5. Microwave emissivities determined from in-situ measurements made during NORSEX.

6. Location of the NORSEX flight tracks along which the data in Figures 7 and 8 were obtained.

7. Comparison of retrievals of C from Nimbus-7 SMMR using various algorithms and also data obtained on board the NASA C-130 during NORSEX.

8. Same as Figure 7, but along different flight tracks.

9. Snow/ice interface temperature vs. snow surface temperatures showing results from the Maykut-Untersteiner model (1971) and a least-squares fit to Ramseier's Pond Inlet data.

Appendix A

SMMR Sea Ice Workshop

Participants

William J. Campbell†	USGS, University of Puget Sound
Mark Anderson	CIRES/University of Colorado
Bob Bindschadler	NASA/GSFC/Code 912.1
Frank Carsey*	JPL/Code 183-501
Don Cavalieri*	NASA/GSFC/Code 912.1
Joey Comiso*	NASA/GSFC/Code 912.1
Per Gloersen*	NASA/GSFC/Code 912
Dick Larson	ERIM, Ann Arbor, MI
Robert G. Onstott	University of Kansas/Remote Sensing Lab.
Anne Owens*	Ph.D. Associates
Claire Parkinson	NASA/GSFC/Code 912.1
Rene' O. Ramseier*	AES/Ice Center, CANADA
Irene Rubinstein*	Ph.D. Associates, Toronto CANADA
Einar Svendsen*	University of Bergen, NORWAY
Calvin Swift*	University of Massachusetts
Bob Thomas	NASA HQ
Ballard Troy*	NRL/Code 7911
Norbert Untersteiner	University of Washington
Jay Zwally	NASA/GSFC/Code 912.1

† Chairman, First SMMR/NET Sea Ice Workshop.

* Gave overview presentations of specific experimental data sets.

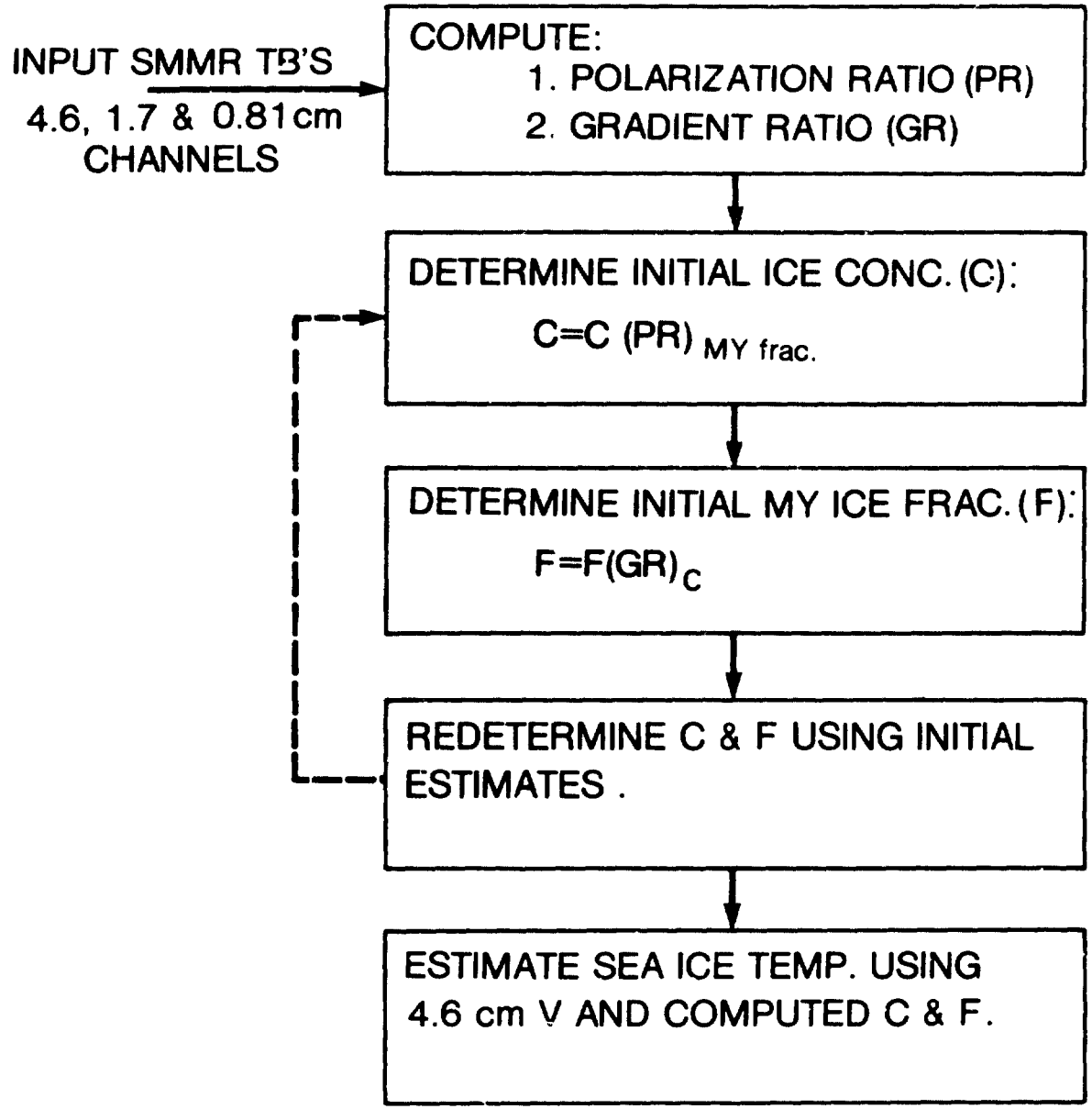
INPUT SMMR TB'S
4.6, 1.7 & 0.81cm
CHANNELS
COMPUTE:
1. POLARIZATION RATIO (PR)
2. GRADIENT RATIO (GR)
DETERMINE INITIAL ICE CONC. (C):
C=C (PR) MY frac.
DETERMINE INITIAL MY ICE FRAC. (F):
F=F(GR)C
REDETERMINE C & F USING INITIAL ESTIMATES .
ESTIMATE SEA ICE TEMP. USING 4.6 cm V AND COMPUTED C & F.

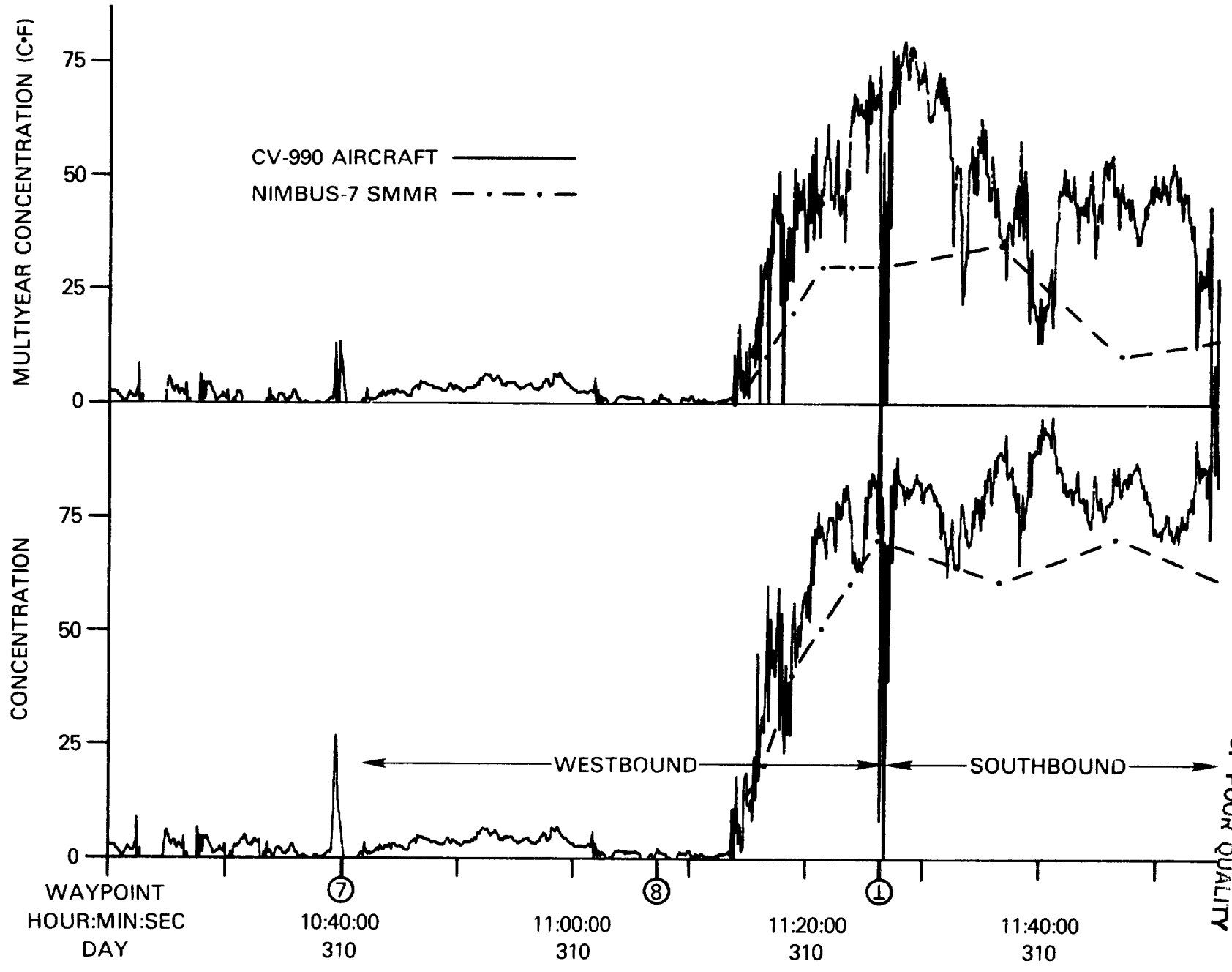
MULTIYEAR CONCENTRATION (C•F)
75
50
25
0
CV-990 AIRCRAFT
NIMBUS-7 SMMR
CONCENTRATION
75
50
25
0
WESTBOUND
SOUTHBOUND
WAYPOINT
HOUR:MIN:SEC
DAY
⑦
10:40:00
310
⑧
11:00:00
310
①
11:20:00
310
11:40:00
310
OF POOR QUALITY

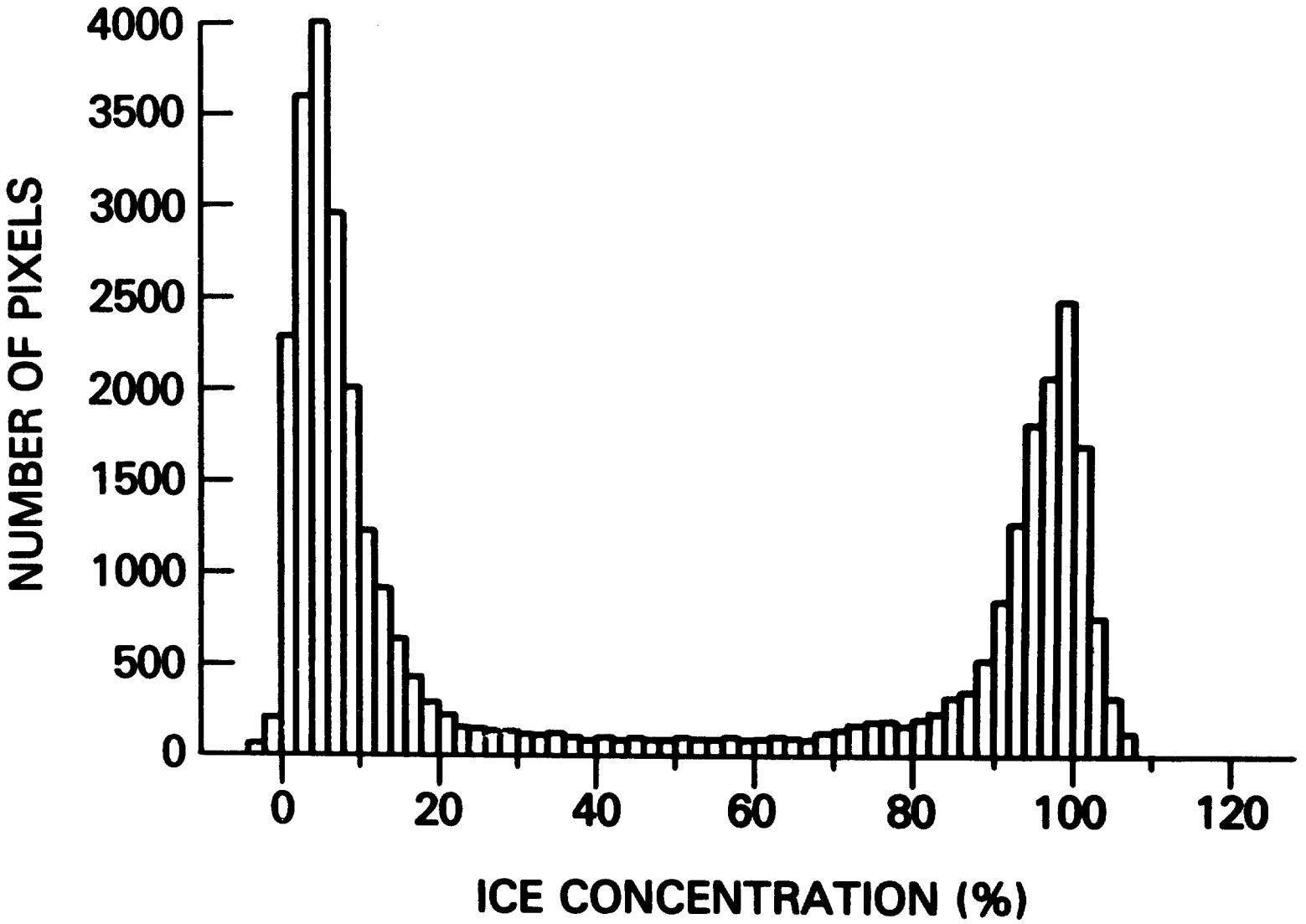

ORIGINAL PAGE IS
OF POOR QUALITY

CAL SWIFT ICE MODEL Ph.D. Feb/82

$$FRAC_{WATER} = \frac{\dfrac{(T_B^{18} - 13)(E_{FY} - E_{MY})^{37}}{(T_S - 12)} - \dfrac{(T_B^{37} - 26)(E_{FY} - E_{MY})^{18}}{(T_S - 26)} - E_{FY}^{18}(E_{FY}-E_{MY})^{37} - E_{FY}^{37}(E_{FY}-E_{MY})^{1}}{(E_{FY} - E_W)^{37}(E_{FY} - E_{MY})^{18} - (E_{FY} - E_W)^{18}(E_{FY} - E_{MY})^{37}}$$

$$FRAC_{MY} = \frac{E_{FY}^{37} - \dfrac{(T_B^{37} - 26)}{(T_S - 26)} - (E_{FY} - E_W)^{37} * FRAC_{WATER}}{(E_{FY} - E_{MY})^{37}}$$

$$FRAC_{FY} = 1 - FRAC_{WATER} - FRAC_{MY}$$

ORIGINAL PAGE IS OF POOR QUALITY

ORIGINAL PAGE IS
OF POOR QUALITY

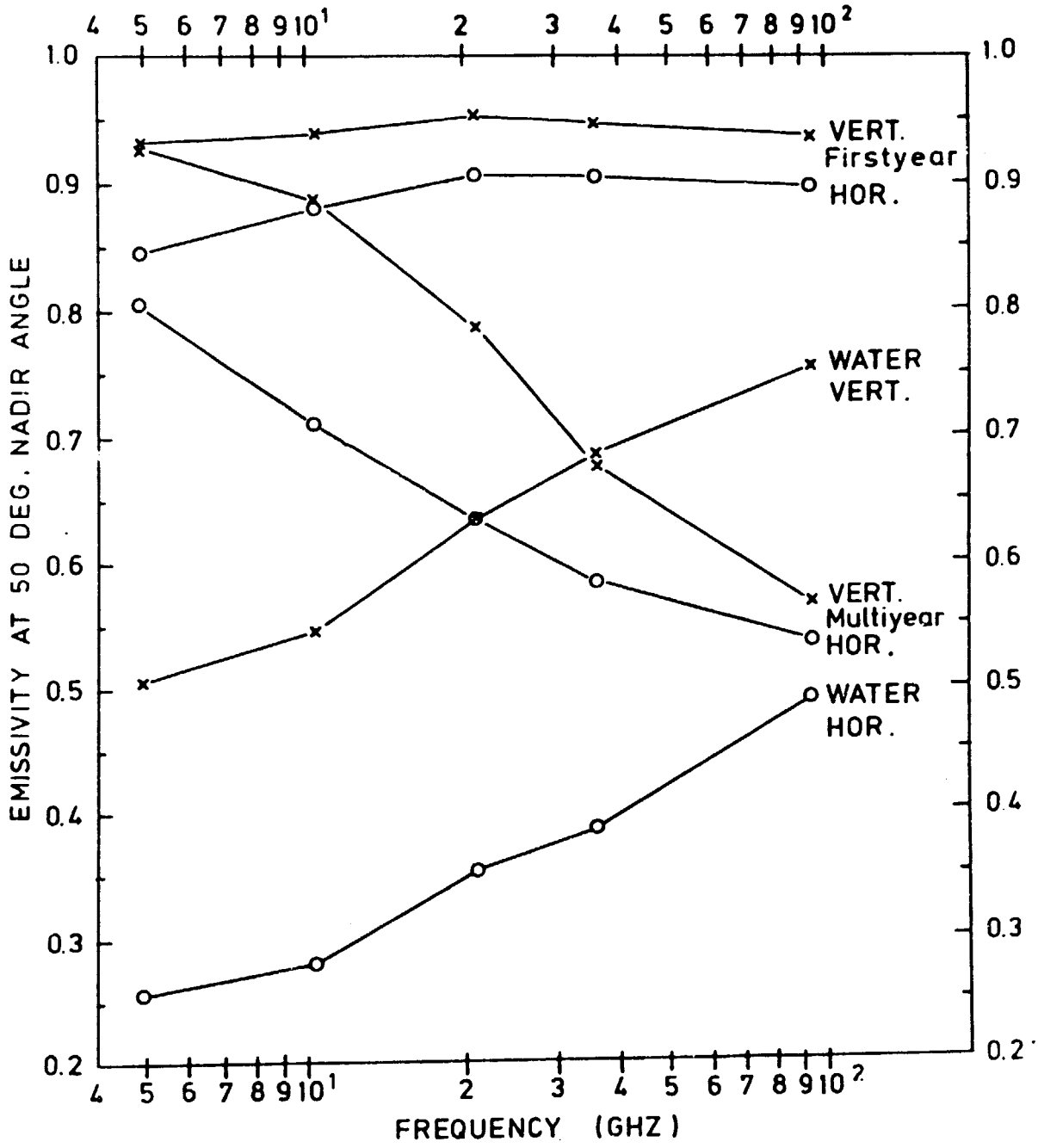

ORIGINAL PAGE IS
OF POOR QUALITY

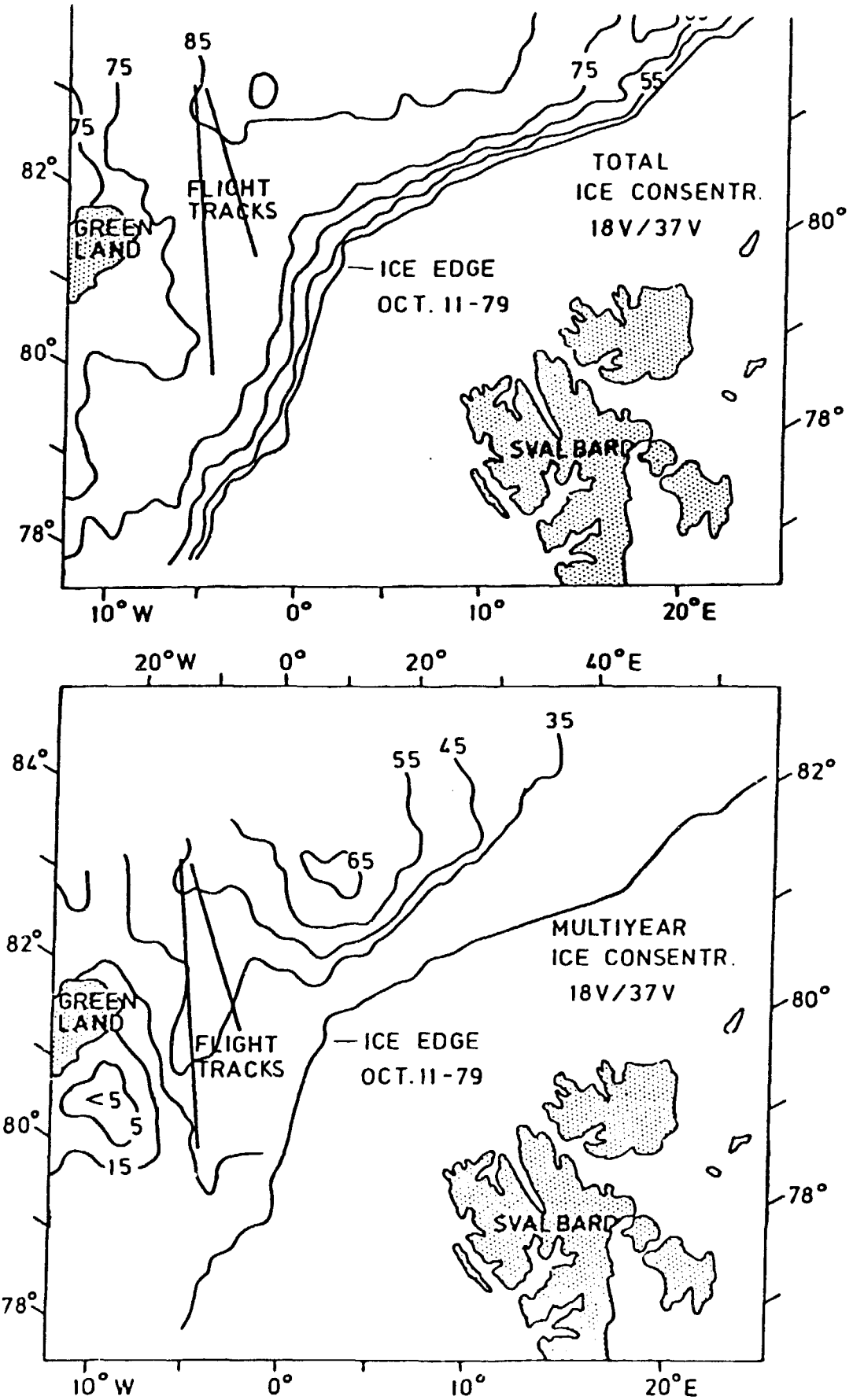

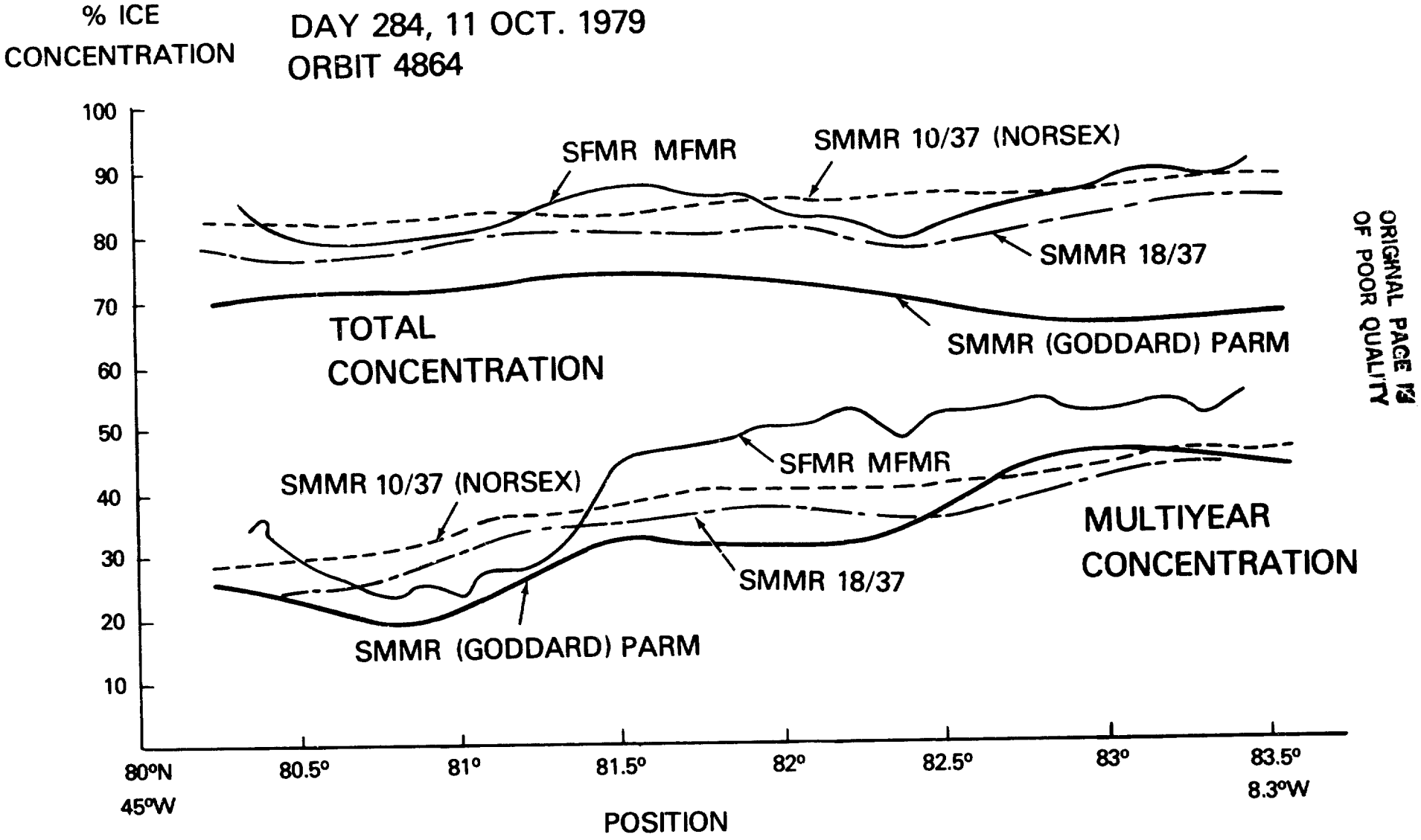

ORIGINAL PAGE IS OF POOR QUALITY

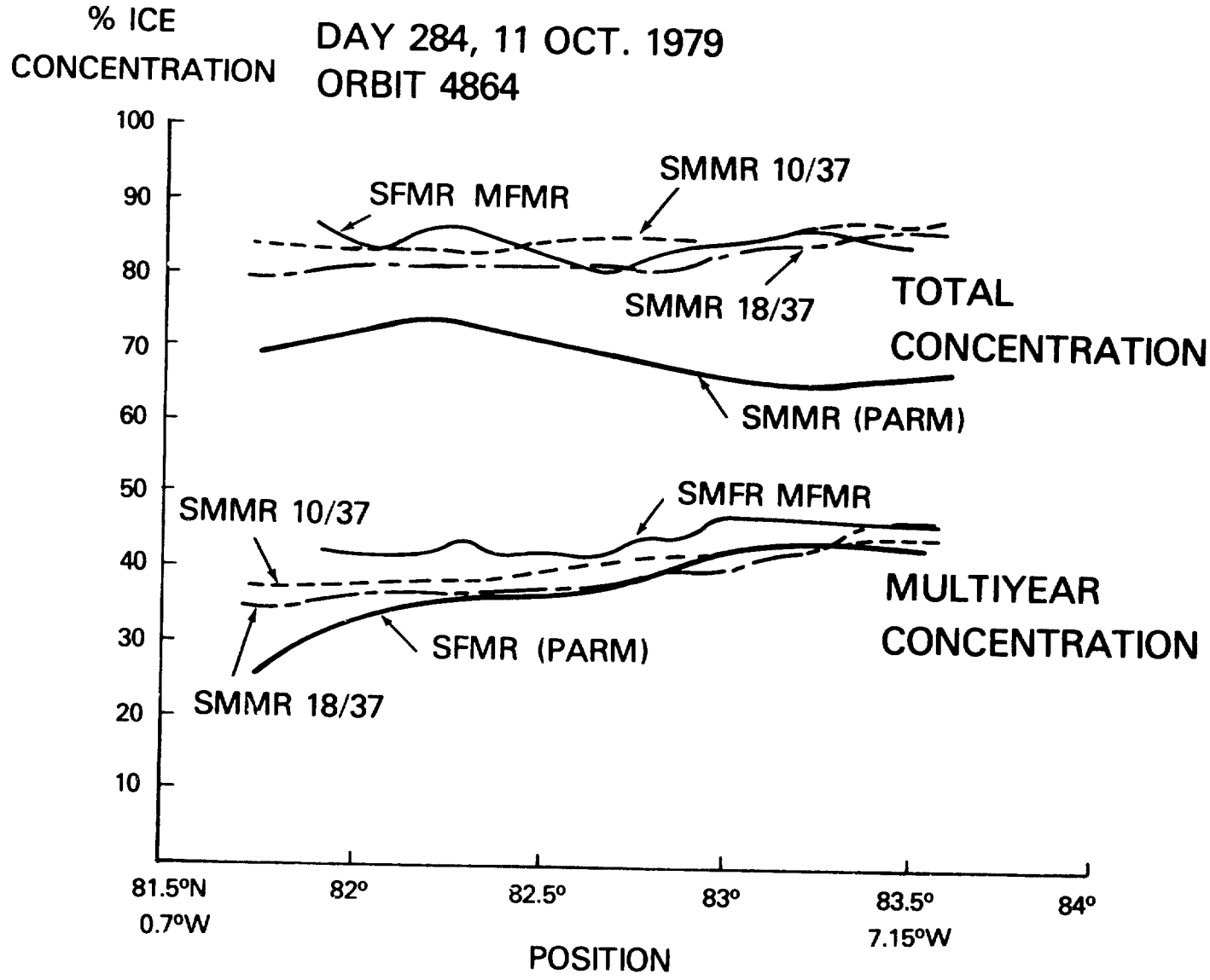

ORIGINAL PAGE IS
OF POOR QUALITY
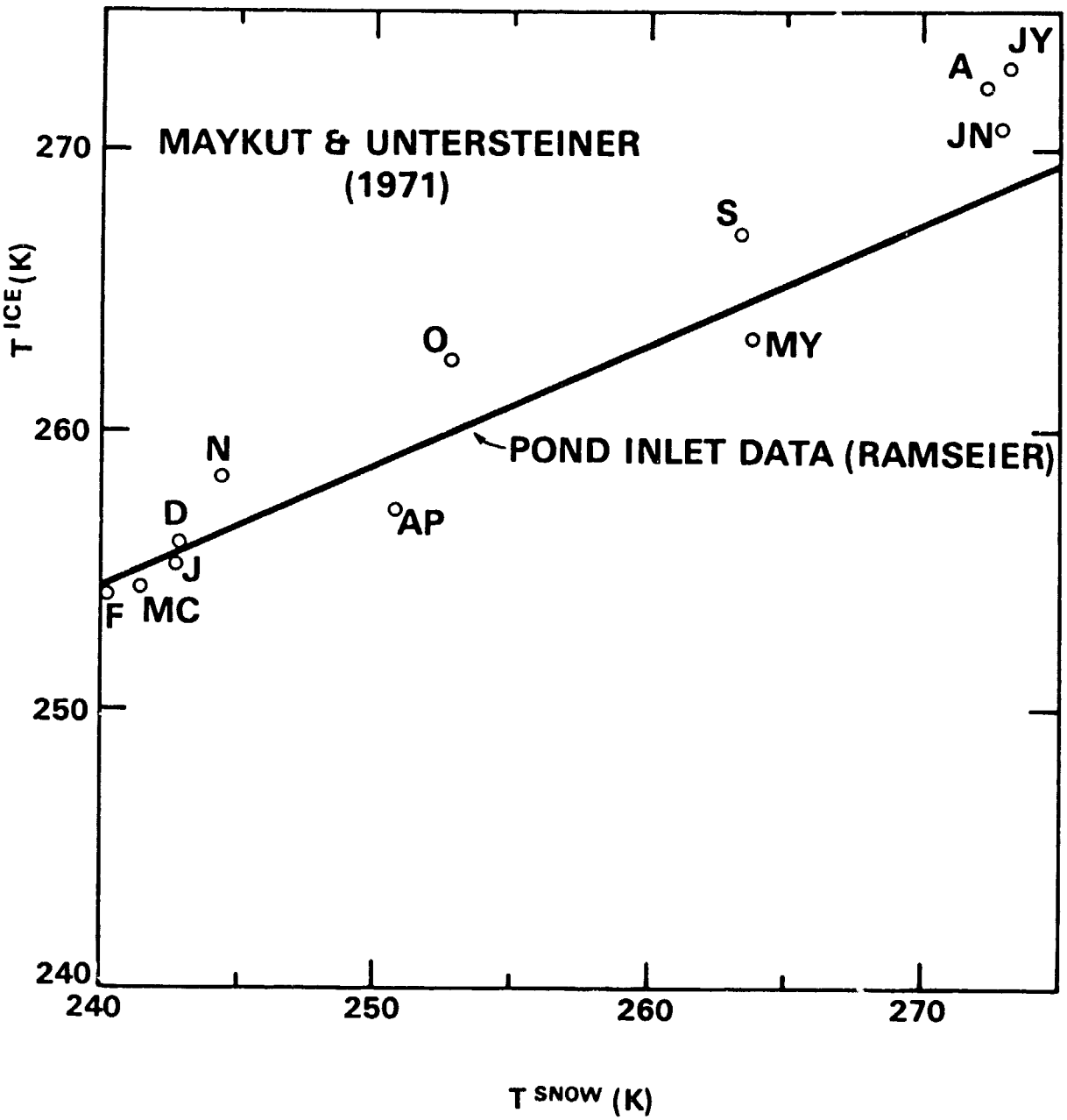
ORIGINAL PAGE IS
OF POOR QUALITY